# Transitions between Elongated Conformations of Ubiquitin [M+11H]$^{11+}$ Enhance Hydrogen/Deuterium Exchange

Brian C. Bohrer, Natalya Atlasevich, and David E. Clemmer*

Department of Chemistry, Indiana University, Bloomington, Indiana 47405, United States

ABSTRACT: Hydrogen/deuterium (H/D) exchange reactions between different elongated conformations of $[M + 11H]^{11+}$ ions of ubiquitin and D_2O are studied by a combination of ion mobility spectrometry (IMS) and mass spectrometry techniques. Three conformers (B, C, and D), resolved in the IMS separation, each exchange ~27 hydrogens upon exposure to 0.06 Torr of D_2O vapor for ~35 to 40 ms. However, a region of the IMS spectrum that appears between the C and D states (corresponding to ions that undergo a structural transition during the mobility separation) undergoes substantially more exchanges (~39 total sites, 44% more than the B, C, and D states). Selection and activation of the individual B, C, and D states reveals that the increased H/D exchange occurs during the transition between structures. Overall, these studies suggest a key process in establishing the maximum exchange levels involves structural transitions, which allow protected sites to be exposed for some fraction of the reaction time. Analysis of changes in exchange levels upon structural transitions can provide insight about common regions of structure that exist in the B, C, and D conformations.
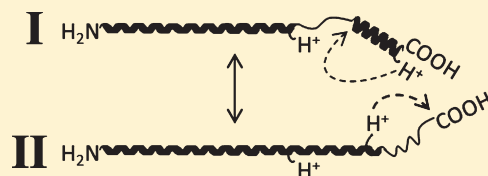
■ INTRODUCTION

Since the development of electrospray ionization[1] for mass spectrometry (MS), several MS-based approaches have been developed for characterizing structures of gas-phase protein ions. These can be categorized as either *chemical* or *physical* methods.[2] Chemical methods include: ion—ion[3,4] and ion—molecule reactions,[5,6] detection of noncovalent adducts,[7—9] and monitoring of hydrogen/deuterium (H/D) exchange[10—12] upon exposure of ions to deuterated solvents. Physical methods include: monitoring products of dissociation, induced by collsional-[13] or photo-excitation[14] or electron capture;[15—17] determination of ion shapes by ion mobility spectrometry (IMS) measurements;[18] and microscopy studies of hillocks formed upon ions hitting surfaces at high energies.[19] Although structural information with atomic precision is not accessible, information from different methods provides insight about the number of favored states, their overall shapes, and pathways connecting them.

In the present work, we use a combination of IMS and H/D exchange measurements to study structural transitions of $[M + 11H]^{11+}$ ions of bovine ubiquitin. The mobilities of ions depend upon their collision cross sections.[20,21] Thus, IMS measurements can provide direct information about an ion's three-dimensional shape. Relatively small proteins, such as ubiqutin,[6] cytochrome *c*,[22] lysozyme,[23] and apomyoglobin,[24] often unfold with increasing charge state.[25] The elongated states that persist over extended time periods (milliseconds to seconds) in the gas phase are favored because such structures minimize repulsive columbic interactions.[26] Recently, IMS—IMS instrumentation[27,28] has been developed specifically to study structural transitions. With this approach, a mixture of conformations can be separated in an initial drift region. A narrow range of conformers having a defined mobility are then selected and exposed to energizing collisions so that new

populations of states are produced. These new structures are subsequently separated in a second IMS drift region. Such an approach makes it possible to follow folding and unfolding transitions in some detail.[28,29]

We focus on ubiquitin in this work because it is a relatively small model system that has been the subject of numerous experimental studies, including H/D exchange,[10,30—33] IMS and IMS—IMS,[28,34—38] and dissociation studies.[16] Bovine ubiquitin is comprised of 76 amino acid residues and has 144 exchangeable heteroatom hydrogen sites. Its sequence is identical to that of human ubiquitin.[39] The $[M + 11H]^{11+}$ charge state favors elongated conformations, having little or no tertiary structure.[28] In their earliest studies, McLafferty and co-workers exposed the ubiquitin ions to 10^{-7} Torr of D_2O for >1000 s by trapping the ions in a Fourier transform (FT) ion cyclotron resonance (ICR) cell. They reported a single value of ~50 exchangeable sites for $[M + 11H]^{11+}$ ubiquitin ions.[10] In 1999, Marshall's group published a FT-ICR mass spectrum for the $[M + 11H]^{11+}$ state of ubiquitin that provided evidence of two ion populations.[30] The largest population of ions exchanged ~60 sites; a smaller fraction of ions underwent ~80 exchanges.[30] All of these values for the $[M + 11H]^{11+}$ state are far below the maximum number of possible exchanges (144 plus 11 protons); generally, nonreactive sites on elongated states are interpreted as being protected by secondary structural elements through hydrogen bonding.[32] Additionally, the orientation of charged sites on highly extended states may not favor efficient exchange because

heteroatom sites are not in close proximity to the site of protonation, where the H/D exchange process initiates.[11,12,40]

Williams and co-workers measured H/D exchange levels for $[M + 11H]^{11+}$ ions of ubiquitin using a field-asymmetric (FA) IMS device coupled to a FT-ICR mass spectrometer.[31] The compensation voltage scan for $[M + 11H]^{11+}$ ubiquitin ions shows a peak and a broad shoulder, consistent with at least two structures. Subsequent exposure to D_2O in the ICR cell for a period of 40 s revealed three exchange levels (16, 30, and 45 sites). Interestingly, the same three levels of exchange were recorded for all compensation voltages.[31] This result appears to demonstrate the complementary nature of mobility and H/D exchange techniques and suggests that proteins of different cross sections can exhibit similar H/D exchange reactivity (and vice versa).[31]

Koeniger and Clemmer carried out high-resolution IMS–IMS studies for the $[M + 11H]^{11+}$ state and reported evidence for four stable conformers. They refer to these as states A, B, C, and D with published collision cross sections of 1613, 1760, 1879, and 1958 Å[2], respectively.[28] Comparisons with calculated cross sections for trial geometries generated in silico indicate that all these structures correspond to elongated states.[6] Although the IMS distributions are dominated by the C and D states, it is possible to study any of the resolved populations. Selection and activation of resolved conformers shows that each can repopulate some of the other states; this occurs in a precursor-dependent manner, requiring that there are favored pathways between structures.[28] Additionally, regions of the IMS spectrum corresponding to unstable states were observed; upon selection such conformations spontaneously appear at a different mobility, associated with one of the stable A through D states. The existence of unstable populations was recently corroborated using a technique called overtone mobility spectrometry (OMS).[41,42] In these studies $[M + 11H]^{11+}$ ions maintained at ~300 K appear to undergo structural transitions in ~3 to 15 ms; such transitions result in the loss of ion signal between the primary peaks in the OMS frequency spectrum.[43]

As we try to rationalize all of the existing data reagarding the structural properties of protein ions, it is important to understand transitions between states. In this paper, we examine how transitions influence H/D exchange levels for several $[M + 11H]^{11+}$ states. We do this by carrying out H/D exchange reactions inside the drift region of an IMS–IMS instrument.[2] For the $[M + 11H]^{11+}$ ion, we find that H/D exchange is enhanced when ions undergo a structural transition. This characterization shows that different elongated conformers have some regions of accessible (and protected) sites that are common to one another, and some that are different. This suggests that these states are related by differences in charge site position and regions of secondary structure—presumably helices.

■ EXPERIMENTAL SECTION

Background and Instrumental. IMS theory[44] and details of the experimental methods[18] are summarized elsewhere. The experiments described below were carried out using a home-built IMS–MS instrument. A description of an instrument used for these studies has been published;[27] only a brief summary is provided here.

Mobility measurements are initiated by introducing a pulse of electrosprayed ions into a drift tube that is filled with ~3 Torr of 300 K He buffer gas. Ions move under the influence of a weak

electric field (9 V·cm^{-1}) down the axis of the ~3 m drift tube and separate according to differences in collision cross section. Ion funnels[45] positioned along the drift tube refocus the ion beam and reduce ion loss to the inner diameter of the instrument. Drift tube segments between funnels can be operated independently for multidimensional analyses. In these experiments, a repulsive potential at the exit of the first drift tube segment is pulsed down to a common potential for a brief period ($100\ \mu s$) to transmit ions of a particular mobility. Ions are then collisionally heated by applying a high field (>300 V·cm^{-1}) across a 0.3 cm activation region immediately preceding the adjacent drift tube segment. Upon entering the second drift tube, ions are rapidly cooled to the temperature of the He buffer gas. In this way, specific mobility-selected ions can be isolated and activated to produce a distribution of product states. These new states are then separated in the remaining drift tube region. A funnel at the exit of the final drift region refocuses the ions through a differential pumping region and into the source of a time-of-flight (TOF) mass analyzer. Data is collected in a nested fashion[29,46] such that drift times are recorded in increments of TOF experiments (maximum flight time of 65 μs). Experimental drift times can be converted to collision cross sections using the relationship

$$\Omega = \frac{(18\pi)^{1/2}}{16}\frac{ze}{(k_B T)^{1/2}}\left[\frac{1}{m_I}+\frac{1}{m_B}\right]^{1/2}\frac{t_D E}{L}\frac{760}{P}\frac{T}{273.2}\frac{1}{N} \quad (1)$$

where ze refers to the charge of the ion, E is the strength of the applied electric field, L is the length of the drift tube, t_D is the measured drift time, and m_I and m_B are the masses of the ion and buffer gas, respectively. Experimental parameters T, P, and N refer to the temperature, pressure, and number density of the buffer gas, respectively, and k_B is Boltzmann's constant.

Theoretical Cross-Section Calculations. The polypeptide sequence of bovine ubiquitin was read into Insight II molecular modeling software (Accelrys Inc., San Diego, CA) on a Unix workstation and was manipulated into a hypothetical, entirely α-helical structure. The atomic coordinates of this structure were then submitted MOBCAL[20] to calculate the collision cross-section for this structure according to the exact hard sphere scattering (EHSS) approximation.[47]

H/D Exchange. D_2O (99.9% purity, Cambridge Isotope Laboratories, Andover, MA) was further purified through three freeze–pump–thaw cycles prior to use. It is then doped into the drift tube from an evacuated flask through a leak valve, mixing with He gas at a tee junction prior to entering the drift tube. Typical partial pressure for these experiments is 0.06 ± 0.01 Torr D_2O. For the drift times associated with the $[M + 11H]^{11+}$ state of ubiquitin studied here, this results in a pressure–time product of ~2.4×10^{-3} Torr·s, which appears to be sufficient to effectively saturate fast-exchanging sites. Cross-section measurements from mixed buffer gas experiments are calibrated to values collected in He for comparison.

Electrospray Conditions. A solution of bovine ubiquitin (90% purity, Sigma Aldrich, St. Louis) was prepared at a concentration of 2.9×10^{-5} M in 60:40:2 (% volume) methanol:water:acetic acid. A syringe pump (KD Scientific, Holliston, MA) was used to send the solution through a pulled capillary tip (100 μm i.d. × 360 μm o.d.) biased ~2.5 kV above the drift voltage at a flow rate of 0.25 μL·min^{-1}.

4510

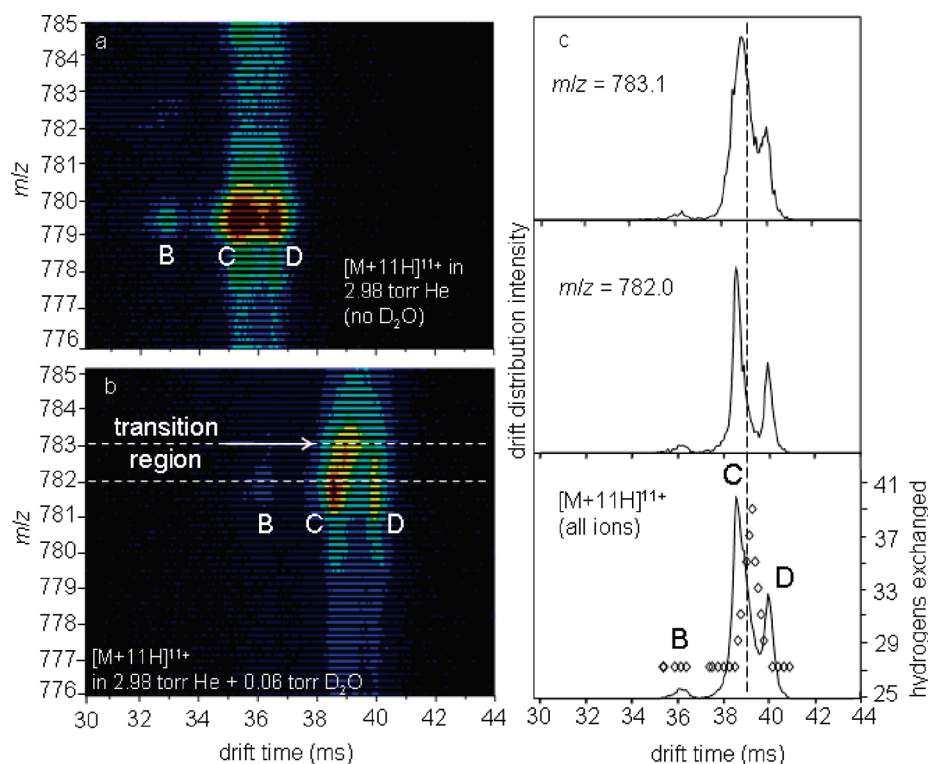dx.doi.org/10.1021/jp2008495 |J. Phys. Chem. B 2011, 115, 4509–4515

Figure 1. IMS−MS plot for the $[M + 11H]^{11+}$ ion of ubiquitin (a) and upon addition of D_2O (b) with states B, C, and D labeled. Integration across $m/z = 781.5−783.5$ obtains the drift distribution in the bottom panel (c), and the open diamond data points correspond to the H/D exchange data points for different drift times. The middle and top panels (c) show the drift distribution for ions exhibiting different levels of exchange (bottom and top dashed lines in 1b), respectively.

■ RESULTS AND DISCUSSION

Example IMS−MS Distributions for Ions Exposed to D_2O. Figure 1 shows example IMS−MS data sets for $[M + 11H]^{11+}$ ions of ubiquitin. In the first case, ions have drifted through 2.98 Torr of pure He at 300 K. The second panel shows results obtained upon addition of 0.06 Torr D_2O to the He gas. The He-only spectrum shows three well-resolved features at $m/z = 779.6$, having drift times that are centered at ∼33.0, 35.5, and 36.5 ms, respectively. Using eq 1 we determine cross sections of 1745, 1870, and 1960 Å^2 for these peaks. The cross sections for the two abundant features are in good agreement with values reported previously for the C ($\Omega = 1879$ Å^2) and D ($\Omega = 1958$ Å^2) states. The smaller feature is consistent with the B state, having a previously reported value of $\Omega = 1760$ Å^2. The A state, which was previously observed (at low abundance), is not observed in these experiments.[28] Upon addition of small amounts of D_2O to the buffer gas, each of these peaks shifts to slightly longer drift times. This systematic shift of all peaks with increasing water vapor pressure occurs because the mobilities of all structures are lower in D_2O than in He.[2] Studies at many partial pressures of D_2O show no evidence for changes in structure due to the presence of D_2O. This is consistent with previous findings.[2]

In addition to changes in the mobilities of ions, the peaks that are observed also shift to higher m/z values as the corresponding ions substitute some ^1H atoms with ^2H isotopes. When combined with the charge state, the m/z shift shows that the B, C, and D states exchange similar numbers of sites. Unlike some dissociative methods,[48] this experiment does not provide information about the location of exchange sites. Therefore, it is possible

that although the three conformations exchange to the same extent, each conformation may differ in which sites exchange. We note that one region of the IMS spectrum does appear to exchange to a different level. Ions found from 38.5 to 39.5 ms exhibit a substantially higher H/D exchange level.

To show these similarities and differences in more detail, consider the insets in Figure 1 which display several integrated IMS distributions. By extracting the two-dimensional data over $m/z = 781.5−783$, we obtain the full drift time distribution for these ions. Extraction of mass spectral data over a narrower range (±0.2 m/z units) provides IMS distributions for specific exchange levels. We estimate the uncertainties in the number of exchange sites (from multiple measurements as well as our ability to determine the peak center in the m/z dimension) to be ±2. The main features in these data at $m/z = 782.0$ (corresponding to 27 ± 2 exchange sites) are three peaks corresponding to the B, C, and D states. As noted above, the region between states C and D undergoes substantially more exchanges, ∼39 ± 2. The peaks associated with the C and D states appear sharper in the narrow slice centered at $m/z = 782.0$ than in the source distribution. This occurs because the region between the peaks exchanges to a different level (and thus appears at a different value of m/z). The narrow slice centered at $m/z = 783.1$ shows a feature between states C and D.

Overall, the improvement in peak resolution observed for different exchange levels lead us to postulate that this occurs because of a transition between structures similar to results published previously.[43] In our OMS study, we found that the C and D states were best resolved at higher overtones.[43] In that report, we speculated that unstable conformations with half-lives

4511

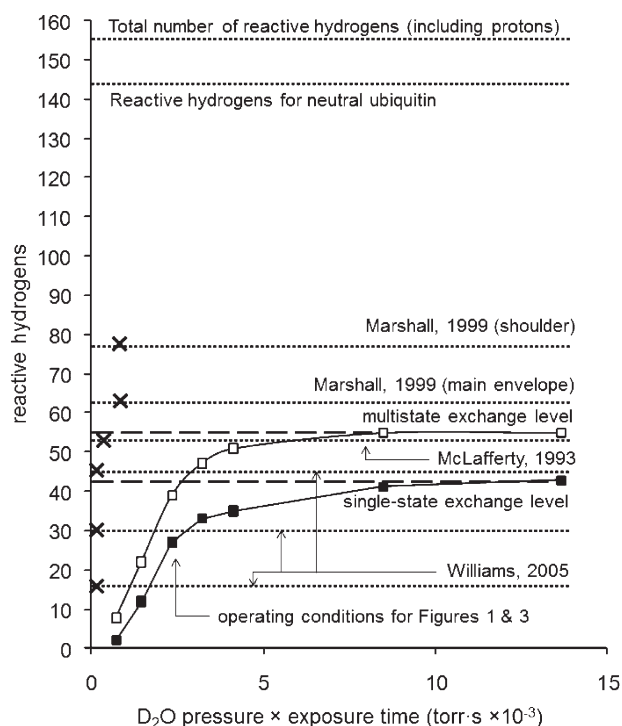dx.doi.org/10.1021/jp2008495 |*J. Phys. Chem. B* 2011, 115, 4509–4515

Figure 2. Saturation curves for incorporation of deuterium by $[M + 11H]^{11+}$ ions of ubiquitin. The solid traces in black and white squares correspond to the single-state and multistate exchange levels, respectively. The horizontal dashed line shows that the multistate exchange level saturates at 55 hydrogens, whereas single-state exchange saturates at 43 hydrogens. Dotted lines are provided for comparison to values reported by McLafferty, Marshall, and Williams (refs 10, 30, and 31, respectively), as well as the upper limits of reactive hydrogens. Approximate exposure conditions for the respective lines of reference are indicated by "X".
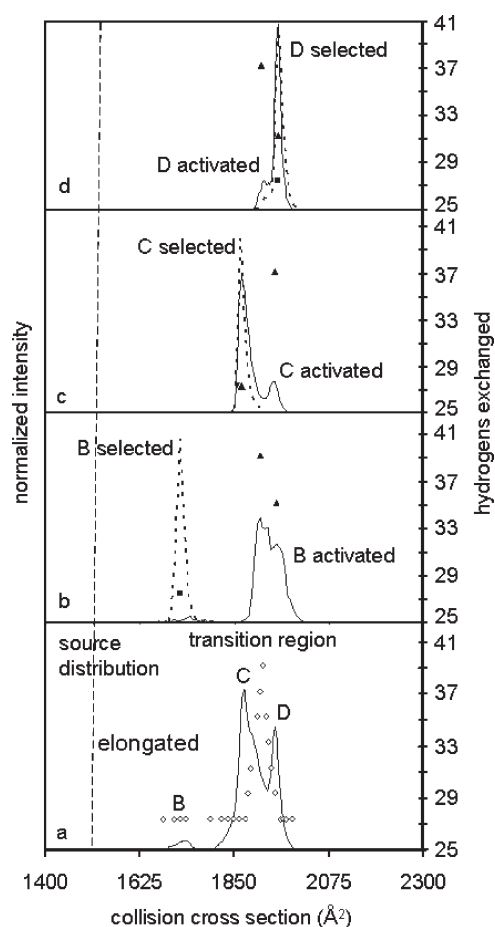

Figure 3. IMS–IMS drift distributions for selection and activation of stable $[M + 11H]^{11+}$ ubiquitin conformers. Panel a shows the source distribution and mobility-resolved exchange data. The next panel up (b) shows isolation of state B in dashed lines and the exchange level of these ions with a square data point. Activation of this conformer yields the distribution and exchange levels indicated by the solid trace and triangle data points, respectively. Similar selections and activations are shown for states C and D (c and d, respectively).

of ∼3 to 15 ms were filtered out of distributions acquired at frequencies that transmit ions at higher overtones.[43]

As expected, the measured level of exchange depends on the D_2O pressure and reaction time. Figure 2 shows a plot of the exchange levels for $[M + 11H]^{11+}$ ions at different partial pressures of the deuterated solvent for 35−53 ms. We refer to the exchange levels measured for the stable B, C, and D peaks as the *single-state* exchange level, and the higher level observed between the C and D peaks as a *multistate* level (because the reactivity corresponds to ions that sample more than one conformation. We plot this on a scale that includes the total reaction time for these ions. This is done so that it is possible to compare the total number of ion-D_2O collisions with values that were obtained by previous FT-ICR studies. Although our reaction times are much shorter than the ICR studies, the total number of collisions is comparable for some measurements reported here.

Figure 2 shows that incorporation of deuteriums increases sharply up to ∼2×10^{-3} Torr·s, corresponding to ∼27 and 39 exchanges for the single-state and multistate levels, respectively. Between ∼2×10^{-3} and 8×10^{-3} Torr·s, deuterium accumulation continues to increase slowly, and above 8×10^{-3} Torr·s, any additional uptake is within the error of the measurement. In this limit, the single-state and multistate exchange levels saturate at 43 and 55 exchanges, respectively. The multistate exchange level is similar to the value of ∼50 reported by McLafferty,[10] and

slightly below the values of 60 and 80 reported by Marshall.[30] The single-state exchange level agrees well with one of Williams' observed distributions,[31] with the other two reported distributions exchanging slightly fewer sites. We note that these exchange levels correspond to ions trapped in ∼8×10^{-7} Torr of D_2O for 40 s, which is by far the least amount of exposure among the studies considered here.

Inducing Structural Transitions. Although there is evidence for an ion population that converts between states C and D, the data presented above is also consistent with an additional structure with a greater H/D exchange reactivity. To investigate this, structural transitions were induced and measured using IMS–IMS experiments. In this approach, mobility-selected precursors are collisionally heated to render a new distribution of product states. If the enhancement of H/D exchange in this system is associated with structural transitions, we would expect the masses of product conformations to increase relative to the masses recorded for different states produced in the source distribution. In Figure 3, the cross-section distribution of ions produced from the source is provided as a reference. IMS–IMS distributions corresponding to selection of states B, C, and D

with no activation show that each selection leads to a distribution that is dominated by a sharp peak. This indicates that most ions do not undergo a structural transition during the remainder of the experiment. We note that selection of the C or D peak shows small populations of ions on the trailing (or leading) side of the main peak. When exposed to 0.06 Torr of D_2O, the exchange level for each selected conformer is measured to be 27, identical to the value reported from Figure 1.

At higher activation voltages, ions are collisionally heated. Although the conditions used here are relatively gentle (100 V over 0.3 cm), far below what is required to induce dissociation, they are sufficient to generate a change in conformation. Figure 3 shows that B state ions undergo a nearly complete conversion to more elongated states. The new states sample a range of cross sections, including a substantial population of D ions, as well as species that appear between the C and D states. Isotopic H/D exchange measurements for the activated ions yield ~39 total sites for species between the C and D peaks. The D state products exchange a total of ~35 sites (increases of 12 and 8 sites, respectively).

Activation of state C results in only a small fraction of ions that undergo a structural transition. The primary product appears to be D state ions. These ions have a measured exchange level of ~37 (~10 additional sites have exchanged). Those ions that remained in the C state upon activation have a measured exchange level of 27. These ions did not change structure or undergo additional exchange. These results are consistent with an interpretation that suggested the increased exchange occurs because ions sample multiple states. It appears that moderate collisional heating does not contribute to increased H/D exchange reactivity unless there is a change in structure. This result also complements experiments by McLafferty and co-workers that induced gas-phase unfolding and refolding of protein ions via collisional and irradiative methods while in the presence of deuterated solvent vapor.[49] In those studies, however, it is unclear the extent to which increased H/D exchange is associated with specific structural transitions (as opposed to other processes, such as scrambling of labeled sites). Finally, activation of D state ions leads to a spectrum in which the leading edge of the selected population is enhanced. This region exchanges ~10 additional sites, a value that is the same as the enhancement measured upon activation of state C. A small increase (~4 sites) is also measured for ions that do not seem to change from the D state. It is possible that these ions briefly sampled a different state before returning to the D state.

Comparison with Previous Results. The multistate exchange level agrees well with the value published by McLafferty,[10] but is still significantly lower than those observed in Marshall's experiments.[30] It seems possible that longer exposure times in FT-ICR MS studies might lead to higher levels of exchange due to transitions between different gas-phase structures. Here, we observe a millisecond time scale transition that appears to be responsible for ~12 additional exchanges; other states may be accessed on longer time scales. FAIMS studies by Williams showed evidence for at least two structures, but H/D exchange data across different compensation voltages appeared similar to one another.[31] Although the FAIMS device may isolate a narrow distribution of structures, the transmitted ions may still undergo structural transitions during the 20—40 s that they are trapped in the ICR cell. Williams' H/D exchange data also showed evidence for three different ion populations. Although our data do not agree quantitatively, the data involving structural transitions

reported here suggest an interesting interpretation of the FAIMS—MS results. The three distributions may correspond to populations that experience different numbers of structural transitions. In this way, the structural history of the ions may be recorded, with those ions that sample the largest number of states appearing as the most heavily labeled.

Implications Regarding Structures. IMS—MS and IMS—IMS—MS studies of H/D exchange reactions of the $[M + 11H]^{11+}$ charge state of ubiquitin indicate the exchange level of these ions is influenced by changes in the ions' structures. Initially, the B, C, and D states exhibit the identical exchange levels. However, when a selected structure is activated and a new structure is formed, the new ions undergo more exchange. This requires that some sites that were initially protected become accessible in the new structure. By selecting and activating an isolated conformer, the extent to which these conformers share common reactive and protected sites can be determined.

It is instructive to consider the changes in exchange levels for specific states in more detail. First consider state B. When B forms states C and D, an increase in exchange level is measured. The new state C undergoes 12 additional exchanges, whereas state D adds only 8 (compared with B). Thus, B has more reactive sites in common with state D than with state C. Next, consider states C and D, which interconvert upon selection and activation. Regardless of whether C converts to D (or vice versa), the number of additional unique reactive sites is the same (~10 additional exchanges). Ions that sample all three states would presumably experience the maximum number of exchanges.

It is interesting to consider the types of structures that are involved in these transitions. From their studies, Oh and McLafferty have proposed that the $[M + 11H]^{11+}$ state of ubiquitin exists as an extended structure comprising multiple networks of $i \rightarrow i + 4$ hydrogen bonding (α-helices).[16] Such extended states are consistent with the large cross sections measured for the A—D ions.[28] That so few sites exchange (27 of 155, only ~17% for the B, C, and D states) also suggests that the majority of sites are highly protected, also consistent with large networked regions of hydrogen bonds. A calculation of the cross section for an entirely helical ubiquitin conformation by the EHSS method leads to a cross section of $\Omega_{EHSS} = 1790$ Å^2 (approximately 4% larger than the experimental cross section for state B and 4—10% smaller than those measured for states C and D). The comparison suggests that we are interrogating ubiquitin conformers comprising substantial α-helical domains. It is likely that the different populations we resolve arise from variations in regions where the helical structure is disrupted. For example, some electrostatic repulsion may lead to fraying in some regions.

To illustrate transitions that would be consistent with our findings, consider Figure 4. This schematic shows two hypothetical structures and a simple transition that allows them to interconvert. This transition ultimately results in changes in the helical and disrupted-helical portions of the polypeptide chain. In this model, we allow the helical and disrupted-helical regions to be influenced by the sites of protonation. It is well-established that protonation can induce helical regions by stabilizing the helix dipole.[50,51] If upon activation, the protonation site configuration changes, then we expect loss of helical structure in the region that was initially charge-capped and induction of a new helical structure in a new region. Such a transition is indicated in the hypothetical structures in Figure 4. Overall, these changes in helix and disrupted-helix configuration still favor elongated structures. Moreover, only a few additional sites
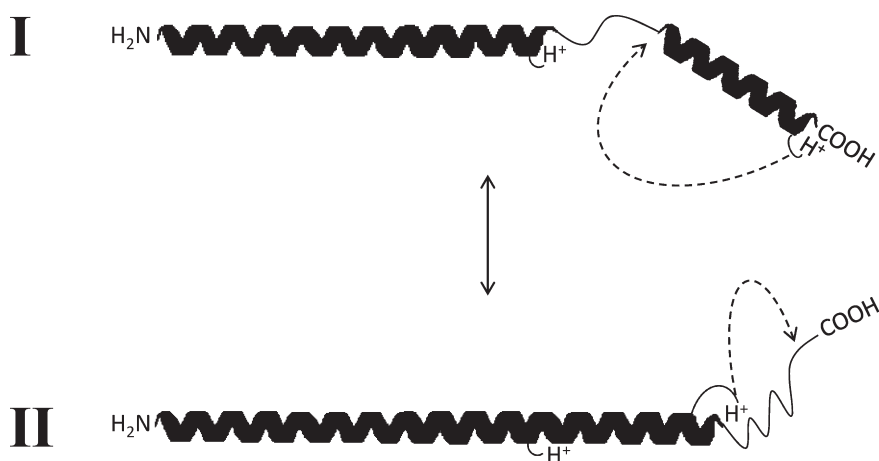
Figure 4. Hypothetical model showing two conformers of ubiquitin $[M + 11H]^{11+}$ ions corresponding to two different sets of protonation sites (**I** and **II**). Helical regions are shown in thick lines with flexible loop regions shown in thin lines. Stabilizing protons are labeled at the C-terminal end of helical regions. Charge migration (shown in dotted arrows) disrupts a helix in **I** while stabilizing a newly formed helical region in **II**.

become accessible for exchange because the total helical content remains high, consistent with our experimental measurements of exchange levels.

CONCLUSIONS

Studies of $[M + 11H]^{11+}$ ubiquitin ions show that H/D exchange levels are enhanced as the result of transitions from one structure to another. This is evident from the two-dimensional IMS—MS nested plot, where the m/z of the ion distribution increases for a mobility region between two previously identified states. Furthermore, ions which are monitored to change their structure by IMS—IMS—MS experiments appear more heavily labeled after the transition. Ion activation alone does not seem to promote H/D exchange in the experiments reported here; activated ions that did not undergo the structural transition exchange few (if any) additional sites. These states appear to correspond to a distribution of charge site configurations, which stabilize helical content along different regions of the conformers. This study provides the first direct evidence for the connection between two conformational states. The measurement indicates that while some regions of the protein are structurally dynamic, other more stable regions are conserved between structures. The results also highlight an important perspective for the interpretation of H/D exchange data. Namely, the experiments reported here indicate that a protein ion exhibiting multiple H/D exchange levels does not necessarily exist in an equal number of stable conformations. Rather, we observe multiple gas-phase conformations for $[M + 11H]^{11+}$ ubiquitin ions, indistinguishable to H/D exchange alone, with the measurable difference resulting from transition between states.

AUTHOR INFORMATION

Corresponding Author
*E-mail: clemmer@indiana.edu.

ACKNOWLEDGMENT

REFERENCES

(1) Fenn, J. B.; Mann, M.; Meng, C. K.; Wong, S. F.; Whitehouse, C. M. *Science* **1989**, *246*, 64–71.

(2) Valentine, S. J.; Clemmer, D. E. *J. Am. Chem. Soc.* **1997**, *119*, 3558–3566.

(3) McLuckey, S. A.; van Berkel, G. J.; Glish, G. L. *J. Am. Chem. Soc.* **1990**, *112*, 5668–5670.

(4) Newton, K. A.; Amunugama, R.; McLuckey, S. A. *J. Phys. Chem. A* **2005**, *109*, 3608–3616.

(5) Gross, D. S.; Schnier, P. D.; Rodriguez-Cruz, S. E.; Fagerquist, C. K.; Williams, E. R. *Proc. Natl. Acad. Sci. U.S.A.* **1995**, *93*, 3143–3418.

(6) Valentine, S. J.; Counterman, A. E.; Clemmer, D. E. *J. Am. Soc. Mass Spectrom.* **1997**, *8*, 954–961.

(7) Schaaff, T. G.; Stephenson, J. L.; McLuckey, S. A. *J. Am. Chem. Soc.* **1999**, *121*, 8907–8919.

(8) Ly, T.; Julian, R. R. *J. Am. Soc. Mass Spectrom.* **2006**, *17*, 1209–1215.

(9) Liu, Z.; Cheng, S.; Gallie, D. R.; Julian, R. R. *Anal. Chem.* **2008**, *80*, 3846–3852.

(10) Suckau, D.; Shi, Y.; Beu, S. C.; Senko, M. W.; Quinn, J. P.; Wampler, F. M.; McLafferty, F. W. *Proc. Natl. Acad. Sci. U.S.A.* **1993**, *90*, 790–793.

(11) Campbell, S.; Rodgers, M. T.; Marzluff, E. M.; Beauchamp, J. L. *J. Am. Chem. Soc.* **1995**, *117*, 12840–12854.

(12) Wyttenbach, T.; Bowers, M. T. *J. Am. Soc. Mass Spectrom.* **1999**, *10*, 9–14.

(13) Loo, J. A.; Edmonds, C. G.; Smith, R. D. *Anal. Chem.* **1991**, *63*, 2488–2499.

(14) Little, D. P.; Speir, J. P.; Senko, M. W.; O'Connor, P. B.; McLafferty, F. W. *Anal. Chem.* **1994**, *66*, 2809–2815.

(15) The interested reader is referred to Zubarev, R. A. *Mass Spectrom. Rev.* **2003**, *22*, 57–77, and articles cited therein.

(16) Oh, H.; Breuker, K.; Sze, S. K.; Ge, Y.; Carpenter, B. K.; McLafferty, F. W. *Proc. Natl. Acad. Sci. U.S.A.* **2002**, *99*, 15863–15868.

(17) Breuker, K.; Oh, H. B.; Horn, D. M.; Cerda, B. A.; McLafferty, F. W. *J. Am. Chem. Soc.* **2001**, *124*, 6407–6420.

(18) For a recent review, see Bohrer, B. C.; Merenbloom, S. I.; Koeniger, S. L.; Hilderbrand, A. E.; Clemmer, D. E. *Ann. Rev. Anal. Chem.* **2008**, *1*, 10.1–10.35.

(19) Reimann, C. T.; Sullivan, P. A.; Axelsson, J.; Quist, A. P.; Altmann, S.; Roepstorff, P.; Velázquez, I.; Tapia, O. *J. Am. Chem. Soc.* **1998**, *120*, 7608–7616.

(20) Meslah, M. F.; Hunter, J. M.; Shvartsburg, A. A.; Schatz, G. C.; Jarrold, M. F. *J. Phys. Chem.* **1996**, *100*, 16082–16086.

(21) Wyttenbach, T.; von Helden, G.; Batka, J. J.; Carlat, D.; Bowers, M. T. *J. Am. Soc. Mass Spectrom.* **1997**, *8*, 275–282.

(22) Clemmer, D. E.; Hudgins, R. R.; Jarrold, M. F. *J. Am. Chem. Soc.* **1995**, *117*, 10141–10142.

(23) Valentine, S. J.; Anderson, J. G.; Ellington, A. D.; Clemmer, D. E. *J. Phys. Chem. B* **1997**, 3891–3900.

(24) Shelimov, K. B.; Jarrold, M. F. *J. Am. Chem. Soc.* **1997**, *119*, 2987–2994.

(25) Badman, E.; Myung, S.; Clemmer, D. E. *J. Am. Soc. Mass Spectrom.* **2005**, *16*, 1493–1497.

(26) Mao, Y.; Woenckhaus, J.; Kolafa, J.; Ratner, M. A.; Jarrold, M. F. *J. Am. Chem. Soc.* **1999**, *121*, 2712–2721.

(27) Koeniger, S. L.; Merenbloom, S. I.; Valentine, S. J.; Jarrold, M. F.; Udseth, H.; Smith, R. D.; Clemmer, D. E. *Anal. Chem.* **2005**, *78*, 4161–4174.

(28) Koeniger, S. L.; Clemmer, D. E *J. Am. Soc. Mass Spectrom.* **2007**, *18*, 322–331.

(29) Pierson, N. A.; Valentine, S. J.; Clemmer, D. E. *J. Phys. Chem. B* **2010**, *114*, 7777–7783.

(30) Freitas, M. A.; Hendrickson, C. L.; Emmett, M. R.; Marshall, A. G. *Int. J. Mass Spectrom.* **1999**, *187*, 565–575.

(31) Robinson, E. W.; Williams, E. R. *J. Am. Soc. Mass Spectrom.* **2005**, *16*, 1427–1437.

(32) Wright, P. J.; Zhang, J.; Douglas, D. J. *J. Am. Soc. Mass Spectrom.* **2008**, *19*, 1906–1913.

(33) Rand, K. D.; Pringle, S. D.; Murphy, J. P.; Fadgen, K. E.; Brown, K.; Engen, J. R. *Anal. Chem.* **2009**, *81*, 10019–10028.

(34) Hoaglund, C. S.; Valentine, S. J.; Sporleder, C. R.; Reilly, J. P.; Clemmer, D. E. *Anal. Chem.* **1998**, *70*, 2236–2242.

(35) Wu, C.; Siems, W. F.; Asbury, G. R.; Hill, H. H. *Anal. Chem.* **1998**, *70*, 4929–4938.

(36) Myung, S.; Badman, E. R.; Lee, Y. J.; Clemmer, D. E. *J. Phys. Chem. A* **2002**, *106*, 9976–9982.

(37) Koeniger, S. L.; Merenbloom, S. I.; Clemmer, D. E. *J. Phys. Chem. B* **2006**, *110*, 7017–7021.

(38) Koeniger, S. L.; Merenbloom, S. I.; Sevugarajan, S.; Clemmer, D. E. *J. Am. Chem. Soc.* **2006**, *128*, 11713–11719.

(39) Schlesinger, D. H.; Goldstein, G. *Nature* **1975**, *255*, 423–424.

(40) Valentine, S. J.; Clemmer, D. E. *J. Am. Soc. Mass Spectrom.* **2002**, *13*, 506–517.

(41) Kurulugama, R. T.; Nachtigall, F. M.; Lee, S.; Valentine, S. J.; Clemmer, D. E. *J. Am. Soc. Mass Spectrom.* **2009**, *20*, 729–737.

(42) Valentine, S. J.; Stokes, S. T.; Kurulugama, R. T.; Nachtigall, F. M.; Clemmer, D. E. *J. Am. Soc. Mass Spectrom.* **2009**, *20*, 738–750.

(43) Lee, S.; Ewing, M. A.; Nachtigall, F. M.; Kurulugama, R. T.; Valentine, S. J.; Clemmer, D. E. *J. Phys. Chem. B* **2010**, *114*, 12406–12415.

(44) Mason, E. A.; McDaniel, E. W. *Transport Properties of Ions in Gases*; Wiley: New York, 1988.

(45) Shaffer, S. A.; Tang, K. Q.; Anderson, G. A.; Prior, D. C.; Udseth, H. R.; Smith, R. D. *Rapid Commun. Mass Spectrom.* **1997**, *11*, 1813–1817.

(46) Hoaglund-Hyzer, C. S.; Lee, Y. L.; Counterman, A. E.; Clemmer, D. E. *Anal. Chem.* **2002**, *74*, 992–1006.

(47) Shvartsburg, A. A.; Jarrold, M. F. *Chem. Phys. Lett.* **1996**, *261*, 86–91.

(48) Pan, J.; Han, J.; Borchers, C. H.; Konermann, L. *J. Am. Chem. Soc.* **2009**, *30*, 91–99.

(49) Wood, T. D.; Chorush, R. A.; Wampler, F. M.; Little, D. P.; O'Connor, P. B.; McLafferty, F. W. *Proc. Natl. Acad. Sci. U.S.A.* **1995**, *92*, 2451–2454.

(50) Counterman, A. E.; Clemmer, D. E. *J. Am. Chem. Soc.* **2001**, *123*, 1490–1498.

(51) Kinnear, B. S.; Hartings, M. R.; Jarrold, M. F. *J. Am. Chem. Soc.* **2002**, *124*, 4422–4431.